

## Ideal MHD stability of ITER steady state scenarios with ITBs

F.M. Poli, C.E. Kessel, S. Jardin, J. Manickam, M. Chance, J. Chen

*Princeton Plasma Physics Laboratory, Princeton, NJ, 08543-0541, USA*

### Introduction

One of ITER goals is to demonstrate feasibility of continuous operations using non-inductive current drive. Two main candidates have been identified for advanced operations: the long duration, high neutron fluency hybrid scenario and the steady state scenario, both operating at a plasma current lower than the reference ELMy scenario [1][2] to minimize the required current drive. The steady state scenario targets plasmas with current 7 – 10 MA in the flat-top, 50% of which will be provided by the self-generated, pressure-driven bootstrap current. It has been estimated that, in order to obtain a fusion gain  $Q > 5$  at a current of 9 MA, it should be  $\beta_N > 2.5$  and  $H > 1.5$  [3]. This implies the presence of an Internal Transport Barrier (ITB). This work discusses how the stability of steady state scenarios with ITBs is affected by the external heating sources and by perturbations of the equilibrium profiles.

Full plasma discharges are simulated with the Tokamak Simulation Code (TSC) [4], a predictive, free boundary transport evolution code that solves the 2D axisymmetric Maxwell-MHD equations on a  $(R, Z)$  grid, coupled to 1D flux surface averaged transport equations for energy and particles. The TSC model includes a 2D representation of the central solenoid and of the poloidal field coils, of the dominant conducting structures and of the feedback systems for plasma position, shape and current.

All simulations begin with a large bore 500 kA plasma, which is grown to full size and shape by  $\sim 14$  s, at which time the plasma is diverted and radio-frequency (RF) heating begins. All plasmas have the same target geometry of  $R = 6.2$  m,  $a = 2.0$  m, elongation  $\kappa \sim 1.8$  and triangularity  $\delta \sim 0.45$ . In the simulations presented herein the current ramp-up time is kept fixed to 150 s and the entire flat-top phase is simulated, until 3000 s. RF heating is used in the earliest phase of the current ramp-up, from 15 s through the whole discharge, while Neutral Beam (NB) heating is used only after the density permissible is reached, approximately half way through the ramp-up. RF sources include Electron Cyclotron (EC) heating, Ion Cyclotron (IC) and Lower Hybrid (LH) current drive. The heating source deposition profiles are calculated offline with TRANSP [5] and then given back to TSC in analytic form. This approach considerably reduces the computational time and it is particularly suitable when studying perturbations of the equilibrium around a reference point, for which trends and scaling with the dominant parameters are searched for.

Particle transport is not modeled in these calculations; the electron density profile and its magnitude are prescribed and the impurity profiles are assumed to be the same as the electron density, with their fraction prescribed. It is assumed a concentration of 2% Berillium and 0.4% Argon, which provide 25-45 MW of core radiated power and bring the conducted power to the divertor to 80-100 MW, within the desired maximum divertor heat flux. Radiation includes bremsstrahlung, cyclotron (Trubnikov model) and line (coronal equilibrium). For steady state scenarios, within the range of plasma currents accessed,  $\sim 7 - 10$  MA, and densities required,  $n_0 \sim 0.65 - 0.75 \times 10^{20} \text{ m}^{-3}$  (with  $n_{ped} \sim 0.5 - 0.67 \times 10^{20} \text{ m}^{-3}$  at  $\rho_{ped} \sim 0.94$ ), the pedestal temperature is predicted with EPED1 to be  $3.3 - 3.7$  keV [6]. A semi-empirical model is used here to model an ITB in the temperature through a modified thermal diffusivity profile, since first-principle theory based transport models have deficiencies when applied to reversed shear plasmas and high pressures.

### Steady state plasma parameters and performance

Five scenarios have been analyzed, including the 2004 baseline configuration with a total external power of 73 MW (33 MW NB and 20 MW each of EC and IC) and four upgrade scenarios with various combinations of NB, IC, EC and LH. Two variations of the baseline scenario are considered, one with doubled EC power, the other with 20 MW IC replaced by the same amount of LH. The last two scenarios use a mixture of 20 MW IC and 40 MW LH, one with 33 MW NB, the other with 8 MW [7]. The plasma current spans between 7 and 10 MA, with nearly 100% non-inductive current driven in all cases and bootstrap fraction  $\simeq 70\%$  in the plasma with 8MW beam and about 50% in the other cases. Central densities are in the range of  $(7 - 8.7) \times 10^{19} \text{ m}^{-3}$ , which correspond to a Greenwald fraction of 0.85 at the largest plasma current and 1.0 at the lowest current. The scenario with 33MW NB+IC+LH has the most peaked pressure profile, with  $p(0)/p = 2.98$  compared to  $p(0)/p = 2.30$  for the same combination of IC+LH at lower beam power, and about 2.6 for the scenarios with EC heating. It also has the highest normalized pressure,  $\beta_N = 2.57$ , and the best performance, with  $Q = 4.6$ . All plasmas have magnetic

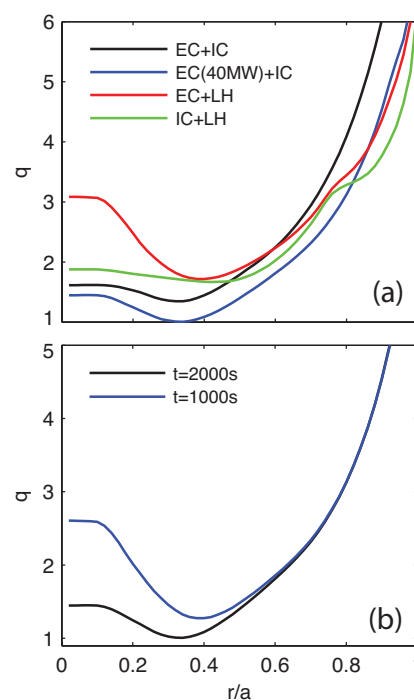


Figure 1: (a) safety factor profile for the scenarios with 33MW NB, at  $t=2500s$ , (b) safety factor for the plasma with 40MW EC, at 1000s and 2500s

shear reversed near the axis, as shown in Fig.1. The  $q$  values decrease during the flat-top until  $t = 2000$ s, when the  $q$  profile reaches complete relaxation. The minimum  $q$  drops below 1.5 in plasmas with IC+EC and it gets close to unity in the case of 40MW EC heating (Fig.1b).

### Ideal MHD stability

The equilibrium solutions calculated with TSC are refined with JSOLVER [8], a fixed-boundary, single fluid, flux-coordinate equilibrium solver. The cartesian coordinates  $(R, Z)$  are treated as functions of the poloidal flux  $\psi$  and poloidal angle  $\theta$  and are iterated on until they satisfy a second-order finite difference approximation to the Grad-Shafranov equation. Ideal kink stability is studied with PEST [9], while large- $n$  ballooning stability is studied with BALMSC [10]. The ideal MHD stability has been analyzed for all scenarios and the sensitivity of these equilibria to a 10% variation of the Greenwald fraction and of the density and temperature peaking factor has been studied. The baseline scenario has low normalized pressure,  $\beta_N \simeq 2.0$ , and it remains stable also with more peaked ITBs, although the minimum safety factor drop below 1.5 in the second half of the current flat-top. Adding 20

MW EC improves the plasma performance ( $\beta_N = 2.4$ ,

$Q = 4.2$ ), but is detrimental for MHD stability because  $q_{min}$  drops to unity at the end of flat-top, causing the formation of sawteeth. Working with broader pressure profiles is beneficial to raise the safety factor, although for this particular plasma the increase in  $q$  is not sufficient to move the equilibrium towards the region of stability. This scenario requires further optimization to freeze the safety factor to values above 1.5. The scenario with EC+LH heating, with  $q_{min} > 1.5$ , has better stability properties even though  $\beta_N = 2.6$  is close to the operational limits. As mentioned in the previous section, the plasma with IC+LH heating has the most peaked pressure profile and the largest  $\beta_N$ . This equilibrium is unstable to high- $n$  ballooning modes during the whole flat-top and it becomes unstable to  $n = 1$  kinks towards the end of the flat-top phase. Figure 2-a shows the solution of the ballooning equation and the eigenfunctions of the  $n = 1$  mode. The curvature (destabilizing) and bending (stabilizing) terms are comparable in absolute value in the

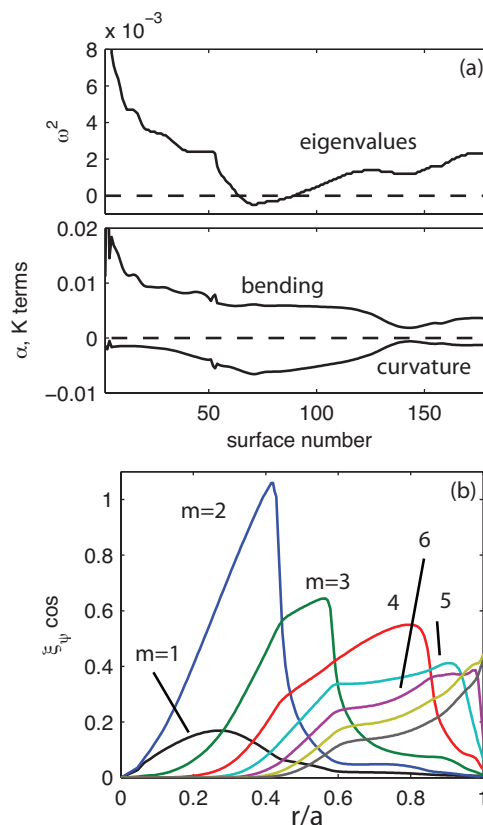


Figure 2: (a) Eigenvalues, stabilizing and destabilizing terms in the ballooning equation; instabilities exist where  $\omega^2 < 0$ . (b) Eigenfunctions of the  $n = 1$  kink mode.

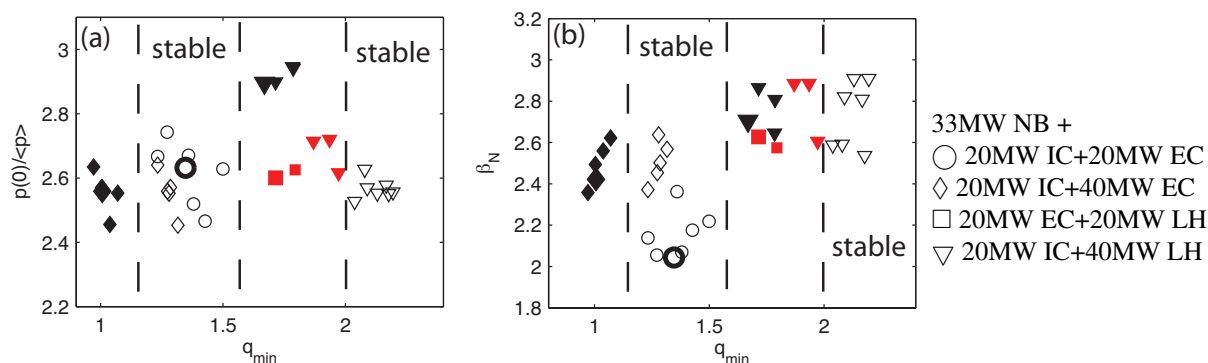


Figure 3: pressure peaking factor (a) and  $\beta_N$  (b) vs  $q_{min}$  for the scenarios with 33MW of beam injection. Empty symbols indicate stable equilibria, red is for ballooning unstable, black means kink unstable.

region of instability, suggesting that small perturbations in the equilibrium, such as variations in the pressure profiles and/or in the current profile may affect the stability of this scenario. The  $n = 1$  kink has multiple harmonics, with a dominant  $m = 2$  component (Fig.2-b); its structure is deeply into the core, making the ITER conforming wall less effective. This plasma can be stabilized by operating with broader ITBs, at  $\rho_{ITB} \geq 0.60$ . The equilibrium is affected in two ways: first,  $q_{min}$  increases above 2, second, the magnetic shear becomes reversed locally outside  $q_{min}$ , where the LH source is more effective in modifying the current profile. Figure 3 resumes the stability properties for the scenarios with 33MW NB. As a general result, MHD unstable equilibria have  $q_{min} < 1.1$ , pressure peaking above 2.8 and  $\beta_N > 2.6$ . Stability significantly improves for  $q_{min} > 2$  (*i.e.* with ITBs sufficiently broad), making possible operations with  $\beta \sim 3$  in the plasma with 10MA current and IC+LH heating. Equivalent equilibria will be investigated for the other scenarios, aiming at optimizing performance close to the operational limits.

**Acknowledgement** This manuscript has been authored by Princeton University and collaborators under Contract Number DE-AC02-09CH11466 with the U.S. Department of Energy. The publisher, by accepting this article for publication, acknowledges that the United States Government retains a non-exclusive, paid-up, irrevocable, world-wide license to publish or reproduce the published form of this manuscript, or allow others to do so, for United States Government purposes.

## References

- [1] Progress in the ITER Physics Basis, Nucl. Fusion (2007) **47**.
- [2] Kessel CE *et al*, Nucl. Fusion (2007) **47** 1274, Kessel CE, *et al*, Nucl. Fusion (2009)
- [3] Green BJ, Plasma Phys. Control. Fusion (2003) **45** 687-706
- [4] Jardin SC *et al*, (1986) J. Comput. Phys. **66** 481.
- [5] TRANSP web site: <http://w3.pppl.gov/transp>
- [6] Snyder P *et al*, Nucl. Fusion (2009) **49** 085035
- [7] Kessel CE *et al*, IAEA Fusion Energy Conference 2010, South Korea.
- [8] DeLucia J, Jardin SC and Todd AMM, J. Comput. Physics (1980) **37** 183
- [9] Grimm RC, Dewar, RL and Manickam J, J. Comput. Physics (1983) **49** 94
- [10] Green JM and Chance MS, Nucl. Fusion (1981) **21** 453. Chance MS, Kessel C and Jardin SC, Plasma Phys. Control. Fusion (1999) **44** 1379